Variation of the magnetic and electrical properties in (1-x)$BiFeO_3$-x$BaTiO_3$ solid solutions

J. PINTEA, A. DUMITRU, D. PATROI, G. SBARCEA, E. MANTA, L. LEONAT
National Institute for Research and Development in Electrical Engineering ICPE-CA, Bucharest, Romania

Multiferroic materials have received a lot of attention lately because of their potential applications for new types of electronic devices (e.g., multiple-state memories and new data storage media). $BiFeO_3$ is a representative multiferroic material which has ferroelectric (Tc = 1103K) and antiferromagnetic (T_N= 643K) properties. In this work, the effect of $BaTiO_3$ content in $BiFeO_3$-$BaTiO_3$ system on the crystal structure, the magnetic properties and the electrical properties have been investigated. The (1-x)$BiFeO_3$ - x$BaTiO_3$ (x = 0.3, 0.4, 0.5) (noted BF-BT) ceramics have been prepared by the solid-state reaction method.

(Received July 14, 2017; accepted November 28, 2017)

Keywords: Multiferroics, Electrical properties, Magnetic properties, $BiFeO_3$-$BaTiO_3$

1. Introduction

Multiferroic materials, exhibiting simultaneously the magnetic and ferroelectric order, have been widely studied in recent years, due to their abundant potential applications in sensors, data storage, spin valve devices, actuators, ultra-high speed telecommunication devices, and spintronics [1-6].

These materials have simultaneous magnetic and ferroelectric activity and even possible attractive functionalities caused by the interaction between the electric polarization and spontaneous magnetization [7-10].

Among the naturally existing oxides, the presence of both ferromagnetism and ferroelectricity is a rare phenomenon, due to the incompatibility between magnetism and ferroelectricity [11-15].

Among the single phase multiferroics, $BiFeO_3$ (BFO) is one of the most extensively studied compound in the latest years because of its spiral spin arrangement and ferroelectric ordering [14-18]. $BiFeO_3$ was proved as ferroelectric with the Curie temperature (T_C) around 1103 K, antiferromagnetic with a high Néel temperature (T_N) of 643K [19], weak ferroelectric/ferromagnetic in some temperature ranges, and also showing a linear magnetoelectric effect [20-23]. But after the preparation of the $BiFeO_3$ solid solution, the impurities phases occur due its formation kinetics. Processing $BiFeO_3$ with other perovskite structured materials, such as $PbTiO_3$, $BaTiO_3$, and PZT, would prevent the formation of secondary phases.

This paper aims to describe the obtainment of the solid solution of the $BiFeO_3$ - $BaTiO_3$ through the addition of the ferroelectric compound $BaTiO_3$ in the $BiFeO_3$ and to study the influence of this chemical composition on the structure and magneto-electric properties.

2. Experiments

The investigated compositions belong to the (1-x) $BiFeO_3$ – x$BaTiO_3$ system, where x = 0.3, 0.4, and 0.5. All three compositions have been synthesized through solid state reactions. For this experiment, the Bi_2O_3, Fe_2O_3, $BaCo_3$ and TiO_2 with purity higher than 99% have been used. The stoichiometric quantities have been weighted and grinded in a humid environment for 8 hours, using mills and agate balls. Water was used to create the humid environment. After drying, the mixed powders have been calcinated at 900^{o}C for 5 hours and then in the wet environment grinded for 8 hours in order to obtain a high homogeneity and to increase the fragmentation degree of the grains. The dry mixtures have been granulated with 4% polyvinyl alcohol 5% concentration of the weight of the material. The mixtures have been pressed with the help of a uniaxial hydraulic press at a pressure of 1200 daN/cm^2, into disk shapes with 12 mm diameter and with a thickness of 2.15 mm. The disks have been sintered at 1050^{o}C for 2 hours in an electric oven type Carbollite, where the temperature presented a linear growth of 5 degrees/minute. In order to determine the electrical properties, the disks have been polished and provided with silver paste electrodes.

The crystal structure of the (1-x)$BiFeO_3$-x$BaTiO_3$ (BF-BT) solid solutions has been examined through X rays diffraction, using a Bruker-AXS diffractometer, type D8 DISCOVER with copper anode. The shape and the size of the grains have been examined through SEM analysis by using the Workstation Auriga scanning electron microscope, produced by Carl Zeiss, Germany. The electrical properties have been measured by means of an Impedance Analyzer (Agilent 4294A) at the ambient temperature within the frequency range of 40 Hz – 30 MHz. The magnetic properties have been measured with the help of the Vibrating Sample Magnetometer (VSM) 7300 Lake Shore for solid samples under magnetic field up to 1.2 T in the ambient temperature.

3. Results and discussions

3.1. Microstructure and crystallographic phase

The X-ray diffraction analysis was performed at ambient temperature and the formation of the desired crystalline structure has been confirmed.

As shown in fig. 1, the XRD patterns show that (1-x)$BiFeO_3$ – x$BaTiO_3$ (x= 0.3, 0.4, 0.5) ceramics crystallize during the perovskite single phase, without the existence of a second phase like pyrochlore. Additionally, all the diffraction peaks were indexed (using ASTM card) for rhombohedral distorted perovskite of R3c space group for x = 0.3 and x = 0.4. For x= 0.5, a cubic structure has been identified. This structure belongs to the spatial group Pm3P. The crystallization in perovskite BF-BT is attributable to the stabilization of the perovskite phase by the formation of a solid solution with $BaTiO_3$.

Our results show that the phase identification presents a rhombohedral symmetry for x = 0.3 and 0.4 respectively and a cubic symmetry for x= 0.5. These results confirm the results presented in the literature [24, 25]. Kumar et al. [26] demonstrate that in (1-x)$BiFeO_3$-x$BaTiO_3$ solid solutions, the phase is rhombohedral for $x \leq 0.3$ and it is cubic when $x > 0.4$.

The apparent density of the prepared ceramic samples has been calculated through the Archimedes method and has the values 7.0518g/cm^3, 6.4725 g/cm^3 and 4.9323 g/cm^3 for x = 0.3, 0.4, 0.5 compositions, respectively.

The lattice parameters obtained through the Rietveld analysis using the specialized software TOPAS, based on the FindIt database, are a = b = 5.643Å and c = 13.828Å for solid solution with x = 0.3, for solid solution with x = 0.4, a = b = 5.648Å and c = 13.837 Å, and also for solid solution x = 0.5, a = b = c = 3.995Å (Table 1).

The computed values of the lattice parameters indicate that there is a continual change of lattice constant as a result of the replacement of the Bi^{3+} ions with Ba^{2+}ions and of the Fe^{3+} with Ti^{4+} ions [27].

SEM analyses were performed on the surface of the sample (fig. 2). The SEM micrographs of all samples shows a heterogeneous microstructure with grain size distribution, consisting of large and small grains. The large grains are probably related to the agglomeration and not to a particular sintering mechanism leading to abnormal grain growth. The $BaTiO_3$ addition influences drastically the microstructure, and thus one can observe the inhibiting effect of the barium titanate which has been used as an additive on the grain growth process and, consequently determines a relative homogenous microstructure, with intergranular porosity and finer grains.

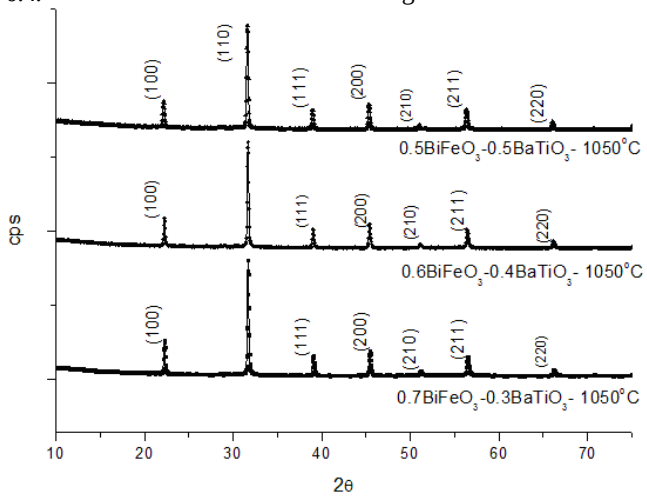

Fig. 1. The XRD diffraction patterns of the solid solutions (1-x)$BiFeO_3$ – x$BaTiO_3$ (x= 0.3, 0.4, 0.5) ceramics sintered at 1050°C temperature

Table 1. Structural parameters of the solid solutions (1-x)$BiFeO_3$ – x$BaTiO_3$ (x= 0.3, 0.4, 0.5) ceramics sintered at 1050°C temperature

Compositions	Associated Structure	Spatial Group	Cell Parameters [Å]		Average size of crystallites [Å]	V^3(Å)	Density (g/cm^3)
0.7$BiFeO_3$ - 0.3$BaTiO_3$ 1050°C -2h	rhombohedral	R3c (161)	5.643	13.828	90.1	381.437	8.171
0.6$BiFeO_3$ - 04$BaTiO_3$ 1050°C -2h	rhombohedral	R3c (161)	5.648	13.837	88.6	382.326	8.152
0.5$BiFeO_3$ - 0.5$BaTiO_3$ 1050°C - 2h	cubic	P3mP	3.995	3.995	89.7	63.779	6.072

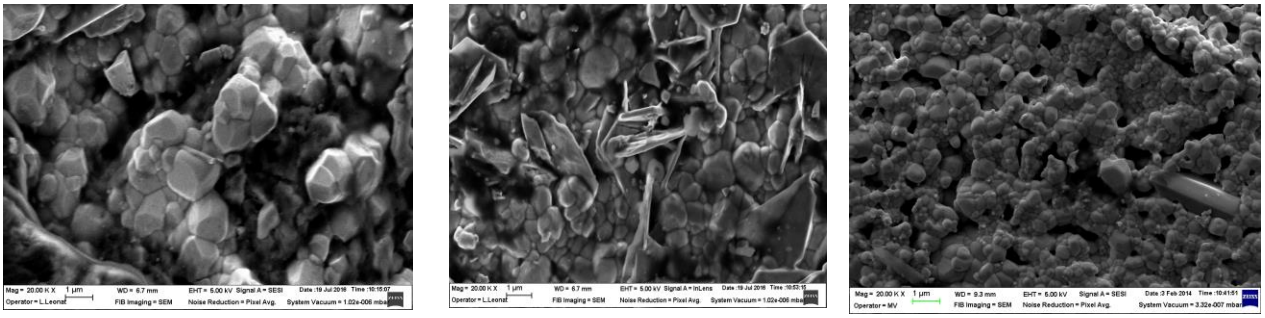

$0.7BiFeO_3$-$0.3BaTiO_3$ $0.6BiFeO_3$-$0.4BaTiO_3$ $0.5BiFeO_3$-$0.5BaTiO_3$

Fig. 2. SEM (scanning electron microscopy) micrographs of the solid solutions (1-x)$BiFeO_3$ – x$BaTiO_3$ (x= 0.3, 0.4, 0.5) ceramics sintered at 1050^{o}C temperature.

3.2. Electrical conductivity

The electrical conductivity is the measure of a material's ability to allow the transport of an electric charge when placed in an electric field**.** The electrical conductivity represents the inverse of the electrical resistivity and for most materials this conductivity strongly depends on the temperature. The resistivity ρ is a fundamental characteristic for any material. The resistivity can be obtained by measuring the resistance of a material with a given geometry. With the help of the following formula:

$$\rho = \frac{U}{I} \cdot \frac{S}{l},$$

the resistivity is computed, where U represents the potential difference measured across the conductor between two points placed at a distance of "l", I is the current through the probe and S represents the area of the probe's section.

From fig. 3, an increase in electrical conductivity with the frequency at room temperature is observed. At the same time, the value of the electrical conductivity of the material decreases with the increase of $BaTiO_3$ concentration.

One can say that by incorporating the $BaTiO_3$ within the $BiFeO_3$ composition, the Fe^{3+} are substituted by the Ti^{4+} and this leads to a reduction of the electric current losses. The result is a decrease of the electrical conductivity by means of an increase of the concentration of the Ti^{4+} ions.

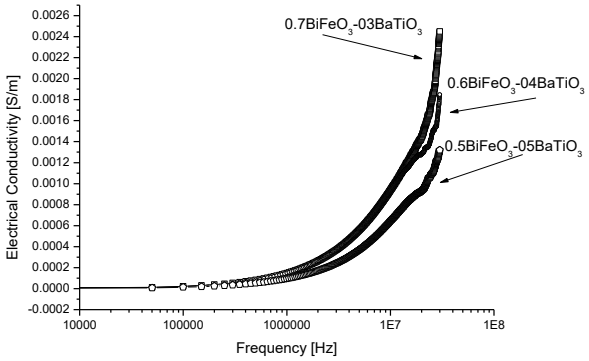

Fig. 3. The variation of the electrical conductivity with the frequency for the system (1-x)$BiFeO_3$-x$BaTiO_3$.

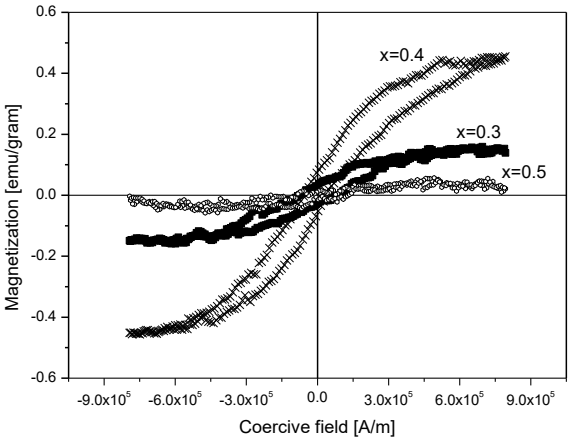

Fig. 4. The hysteresis curves of the probes with x=0.3, 0.4 and 0.5 respectively

3.3. Magnetic properties

The magnetic behavior of the perovskite (1-x)$BiFeO_3$-x$BaTiO_3$ for x = 0.3; 0.4 and 0.5 respectively has been evaluated by using a VSM 7300 type Lake Shore. Fig. 4 shows the M - H hysteresis loops of the sintered solid samples measured at room temperature. The compositions show the typical M - H hysteresis loops of weak ferromagnetism at x = 0.3 and stronger ferromagnetism at x = 0.4. This phenomenon is caused by the structural symmetry arrangement of the compositions, rhomboedral for x = 0.3 and 0.4, and cubic for x = 0.5 [28-30].

One can observe that the remanent magnetization of the composition with x = 0.4 is bigger than the one belonging to the composition with x = 0.3 and it decreases strongly in the case of the composition with x = 0.5. This is due to the decrease of the Fe ions within the composition and thus due to the decrease of the conductibility.

3.4. Electrical properties

The variation of the electrical capacity and of the loss tangent of the ceramic composition (1-x)$BiFeO_3$-x$BaTiO_3$ with x= 0.3, 0,4 and 0.5 respectively is presented in fig. 5a and fig. 5b. It can be observed that for the composition with x= 0.3, the electric capacity presents a peak at 400°C, while for the composition with x = 0.4, these peaks appear moved to the left, it is flattened but it is not a Curie point.

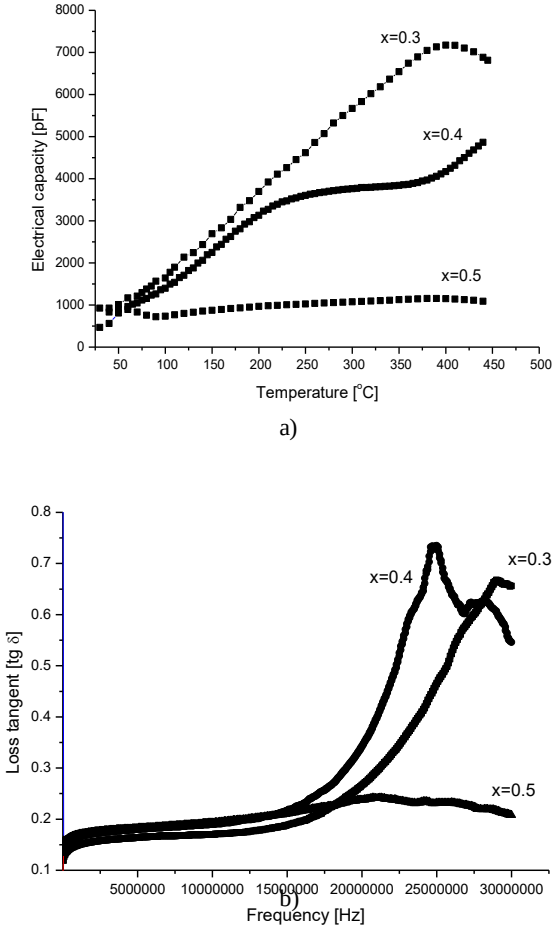

Fig. 5. Electrical capacity of the compositions 0.7$BiFeO_3$-0.3$BaTiO_3$, 0.6$BiFeO_3$-0.4$BaTiO_3$ and 0.5$BiFeO_3$-0.5$BaTiO_3$ during heating

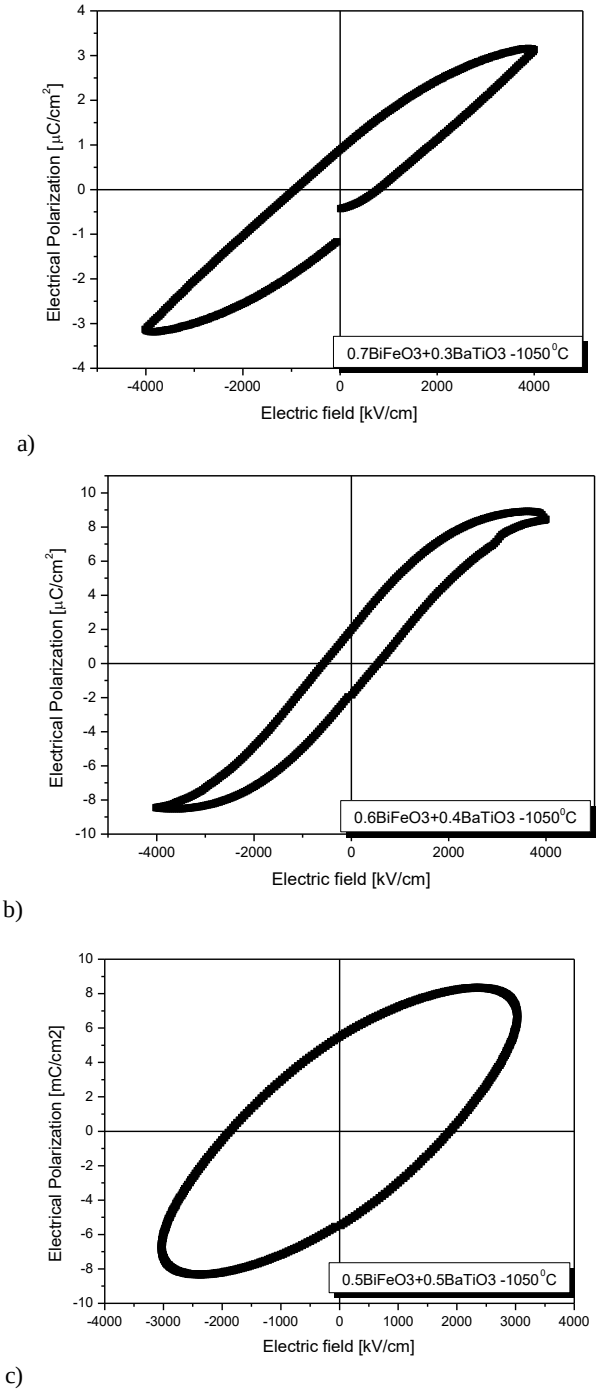

Fig. 6. Hysteresis loops of electrical polarizations vs. E field at room temperature for the compositions a) 0.7$BiFeO_3$-0.3$BaTiO_3$, b) 0.6$BiFeO_3$-0.4$BaTiO_3$ and c) 0.5$BiFeO_3$-0.5$BaTiO_3$.

Fig. 6 shows the P-E hysteresis loops of the (1-x)$BiFeO_3$-x$BaTiO_3$ measured at room temperature. The samples presented typical ferroelectric P - E hysteresis loops when an electrical field of 4000 V and 0.1 Hz frequency has been applied.

The compositions exhibited an increase in remanent polarization with the increase of $BaTiO_3$ content.

Fig. 6a and b presents the variation of the polarization with the variation of the applied electrical field (P-E) on the (1-x) $BiFeO_3$-x$BaTiO_3$ ceramics. This variation has been measured at a frequency of 0.1 Hz at room temperature. The figure shows a growth of the remanent polarization with the growth of the $BaTiO_3$ content.

The results show that the ferroelectric properties can be improved by increasing the $BaTiO_3$ content. This improvement of ferroelectric properties is explained by means of an increased electrical polarization and the reduction of the electric current losses. [15].

4. Conclusions

The perovskit ceramics (1-x)$BiFeO_3$-x$BaTiO_3$ have been prepared through the solid state reaction method. Through this procedure, it was shown that no peaks of impurities appear in the X rays diagram as a side effect of the $BaTiO_3$'s presence. The ferroelectric and ferromagnetic properties of the (1-x)$BiFeO_3$-x$BaTiO_3$ system have been highly changed by the introduction of the $BaTiO_3$. It has also been observed that these properties improve as the $BaTiO_3$ quantity increases, for $x \leq 0.4$.

Acknowledgements

This research was performed with the support of Romanian National Research Program (NUCLEU) nr. 14N/2016, project PN 16110207 - "Researches on ferrous / multiferrous materials for the development of new applications"

References

[1] J. F. Scott, Nature Materials **6**, 256 (2007).
[2] J. Allibe, S. Fusil, K. Bouzehouane, C. Daumont, D. Sando, E. Jacquet, C. Deranlot, M. Bibes, A. Barthelemy, Nano Letters **12**, 1141 (2012).
[3] M. Bibes, A. Barthelemy, Nature Materials **7**, 425 (2008).
[4] Y. Tokura, Science **312**, 1481 (2006).
[5] C. A. F. Vaz, J. Hoffman, C. H. Ahn, R. Ramesh, Advanced Materials **22**, 2900 (2010).
[6] Liu Zhao-Jun, Zhao Jian-Guo, Zhang Wei-Ying, Liu Shi-Jian, J. Optoelectron. Adv. M. **16**(3-4), 340 (2014).
[7] L. Mitoseriu, Bol. Soc. Esp. Ceram. **44**, 177 (2005).
[8] Y. Tokura, J. Magn. Magn. Mater. **310**, 1145 (2007).
[9] C. W. Nan, M. I. Bichurin, S. Dong, D. Viehland, G. Srinivasan, J. Appl. Phys. **103**, 031101 (2008).
[10] Mingwei Zhang, Le Xin, Optoelectron. Adv. Mat. **9(**5-6), 673 (2015).
[11] N. A. Hill, Journal of Physical Chemistry B **104**(29), 6694 (2000).
[12] Y. Tokura, S. Seki, N. Nagaosa, Reports on Progress Physics **77**(7), 076501 (2014).
[13] S. Fusil, V. Garcia, A. Barthelemy, M. Bibes, Annual Review of Materials Research **44**, 91 (2014).
[14] P. Fischer, M. Polomska, I. Sosnowska, M. Szymanski, J. Phys. C. Solid State Phys. **13**, 1931 (1980).
[15] K. Recko, U. Wykowsk, W. Olszewski, G. André, J. J. Milczarek, D. Satuła, M. Biernacka, B. Kalska-Szostko, J. Waliszewski, K. Szymański, J. Optoelectron. Adv. M. **17**(7-8), 1173 (2015).
[16] I. H. Ismailzade, R. M. Ismailov, A. I. Alekberov, F. M. Salaev, Phys. Stat Solidi. A **68**, K81 (1981).
[17] M. M. Kumar, A. Srinivas, S. V. Suryanarayana, J. Appl. Phys. **87,** 855 (2000).
[18] W. M. Zhu, Z. G. Ye, Ceram. Int. **30**, 1435 (2004).
[19] B. Ruette, S. Zvyagin, A. P. Pyatakov et al., Physics Review B **69**, 064114 (2004).
[20] I. H. Ismailzade, R. M. Ismailov, Phys. Status Solidi A **59**, K191 (1980).
[21] P. Fischer, M. Polomska, I. Sosnowska, M. Szymanski, J. Phys. C. Solid State Phys. **13**, 1931 (1980).
[22] I. H. Ismailzade, R. M. Ismailov, A. I. Alekberov, F. M. Salaev, Phys. Stat Solidi. A **68**, K81 (1981).
[23] S. Tanasescu, C. Marinescu, A. Sofronia, A. Ianculescu, J. Optoelectron. Adv. M. **11(**8), 1196 (2009).
[24] Hailong Zhang, Wook Jo, Ke Wang, Kyle G. Webber, Ceramic International **40,** 4759 (2014).
[25] T. H. Wang, C. S. Tu, Y. Ding, et al., Current Applied Physics **11**, S240 (2011).
[26] M. M. Kumar, A. Srinivas, S. V. Suryanarayana, Journal of Applied Physics **87,** 855 (2000).
[27] Hemant Singh, Amit Kumar, K. L. Yadav, Materials Science and Engineering B **176,** 540 (2011).
[28] M. M. Kumar, S. Srinath, G. S. Kumar, et al., Journal of Magnetism and Magnetic Materials **188,** 203 (1998).
[29] H. Singh, A. Kumar, K. L. Yadav, Materials Science and Engineering B **176**, 540 (2011).
[30] M. M. Kumar, A. Srinivas, G. S. Kumar, et al., Journal of Physics: Condensed Matter **11**, 8131 (1999).

*Corresponding author: jana.pintea@icpe-ca.ro